

## 2DH Morphological Modelling of Submerged Breakwaters

S.C. van der Biezen<sup>1</sup>, J.A. Roelvink<sup>1,2</sup>, J. van de Graaff<sup>1</sup>, J. Schaap<sup>3</sup> and L. Torrini<sup>3</sup>

### Abstract

The results are presented of 2DH numerical modelling of morphological effects of submerged breakwaters. In particular, segmented configurations are focussed upon, since segmented submerged breakwaters induce interesting and important current circulations in the horizontal plane.

In a previous study, a module that calculates a phase-averaged stationary wave field was used to compute wave forces. These forces were next used to calculate current patterns. In the present study, waves are introduced via a harmonic boundary condition in a phase-resolving module, based on the nonlinear shallow water equations. The advantage of this approach is that the current patterns are directly calculated, the disadvantage is that it requires more computation time.

The first results of morphodynamic computations with submerged breakwaters, in intra-wave mode, are promising. The most important mechanisms are reproduced rather well. Some of the shortcomings of the previous model study with a stationary wave model have been overcome. However, a lot of fine tuning still needs to be done.

### 1. Introduction

Submerged breakwaters are detached, mostly shore parallel, structures with their crest below water level. Their purpose is twofold. Firstly, submerged breakwaters ‘filter’ waves, by causing larger waves to break and leaving smaller waves more or less undisturbed. Secondly, they block offshore transport of sediment.

In Italy, submerged breakwaters have been used at various locations (Lamberti and Mancinelli, 1996; Tomasicchio, 1996). Their economic and aesthetic (Liberatore, 1992; Ozaki and Mitsuhashi, 1993) advantages compared to emerging breakwaters make submerged breakwaters an attractive tool for coastal management.

However, specially in case of the segmented configuration, one should be prepared for large sediment losses through the gaps due to concentrated offshore flow (Browder et al., 1996). A special (and expensive?) design of the structure may solve

---

<sup>1</sup> Faculty of Civil Engineering and Geosciences, Delft University of Technology, Stevinweg 1, 2628 CN, Delft, The Netherlands, J.vandeGraaff@ct.tudelft.nl

<sup>2</sup> Delft Hydraulics, Delft, The Netherlands, Dano.Roelvink@wldelft.nl

<sup>3</sup> M.Sc. student, Delft University of Technology

this problem (Nobuoka et al., 1996). In any case, extensive numerical and physical modelling are recommended for a proper implementation (Smith et al., 1995).

## 2. Basin experiments

At the Laboratory of Fluid Mechanics of Delft University of Technology, small scale 3D basin experiments with segmented submerged breakwaters were carried out (De Later, 1996; Van der Biezen et al., 1996). Aim of the experiments was to obtain a data-base for numerical modelling studies. A movable bed was used to include morphological effects of the structures. The measurements focussed on morphology rather than on hydrodynamics. Apart from Delft University of Technology, five other universities participated in this research project, which was funded by the Human Capital and Mobility Programme of the EU.

At the Hydraulic and Maritime Research Centre in Cork, Ireland, hydrodynamic parameters were measured in similar tests with a fixed bottom (Murphy et al., 1996). Apart from these basin tests, flume experiments were carried out as well by other universities. Detailed information on the project is included in the Test Definition Report (Høgedal et al., 1994).

### 2.1 Experimental setup

In the wave basin (length = 28 m, width = 14 m, depth = 0.60 m), three series of test were carried out: one series without structures, one series with three separate breakwaters of 6 m length each (two gaps of 3 m in between) and one with two breakwater segments of 12 m and 6 m length with only one gap of 3 m in between. In each series three different wave heights were generated: 0.08 m, 0.10 m and 0.12 m. The generated wave field was regular and normal incident to the beach, with a wave period of 1.55 s. The initial beach slope for each test was 1:15. Figure 1 shows a plan view of the wave basin for the configuration with three submerged breakwaters (all measures in meters).

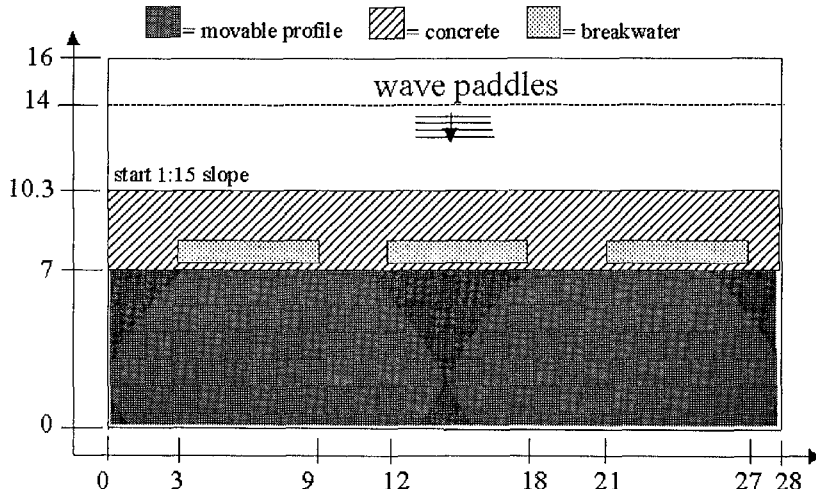


Figure 1. Plan view of the wave basin with three submerged breakwater segments.

All experiments were conducted with a rubble mound breakwater with an impermeable core and 2:3 slopes on both sides. The armour layer of the prototype breakwater consisted of two layers of rock stones,  $D_{50} = 0.812 \text{ m}$ . The crest width was chosen as  $3D_{50}$  and the thickness of the armour layer as  $2D_{50}$ . The water depth at the seaward toe of the breakwater equals 6 m and the breakwater submergence equals 1.5 m.

Scaling the prototype breakwater with a 1:15 ratio yields the measures given in Figure 2. The submergence of the breakwater crest is constant for all tests.

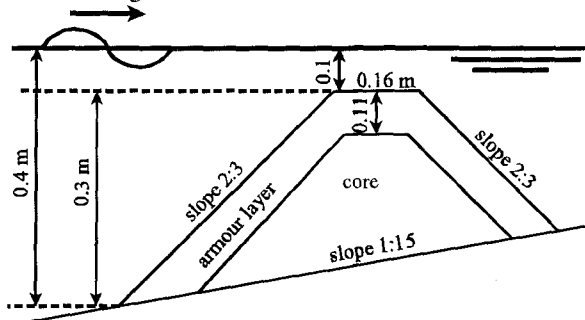


Figure 2. Submerged breakwater design

The structure is placed on a concrete slope. The profile landward of the structure consists of sediment with a grain size  $D_{50}$  of  $95\mu\text{m}$ .

## 2.2 Measured parameters

The experiments lasted 7:30 h each, interrupted by several profile measurements. The first profile measurement is at  $t = 0:00 \text{ h}$ , the initial profile. The next measurements are at  $t = 0:30 \text{ h}$ ,  $t = 1:30 \text{ h}$ ,  $t = 3:30 \text{ h}$  and, finally, at  $t = 7:30 \text{ h}$ . During the profile measurements the wave generator was stopped.

Apart from the profile height, velocities in the horizontal plane and free surface elevations were measured. The time series were taken at different cross-sections. For more details, reference is made to Van der Biezen et al. (1996).

## 2.3 Measurement results

The measurement results presented here only intend to illustrate the measurement data used for the numerical study. For each measured parameter a short explanation is given.

Figure 3 shows two examples of measured wave heights, for a generated wave height of 0.12 m. The left plot shows wave height measurements for an experiment without submerged breakwaters, and the right plot shows measurements in a cross-section with a submerged breakwater.

Free surface elevation was measured at four cross-shore locations. From the time series, an average wave height was calculated using the standard deviation of all samples. Although the hydrodynamic measurements are not detailed, the influence of the submerged structure on the wave heights is clearly visible.

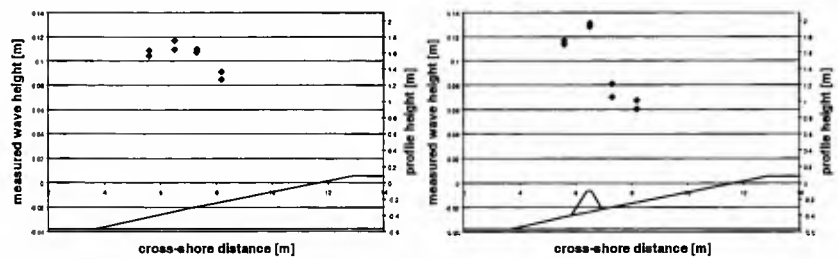


Figure 3. Measured wave heights with and without a submerged breakwater

Current velocities in the horizontal plane were measured at several cross-shore locations. Figure 4 shows depth averaged currents, averaged in time over the first 1:30 h of the experiment to obtain the overall current pattern. The waves propagate top-down in this figure.

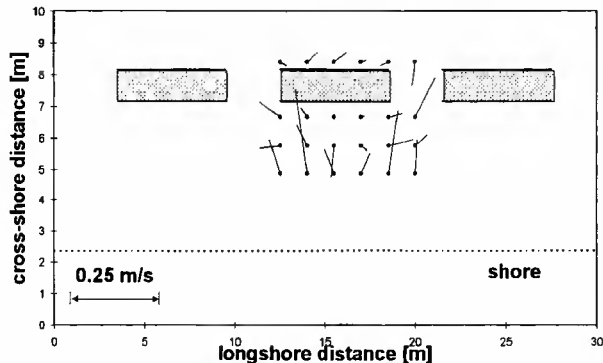
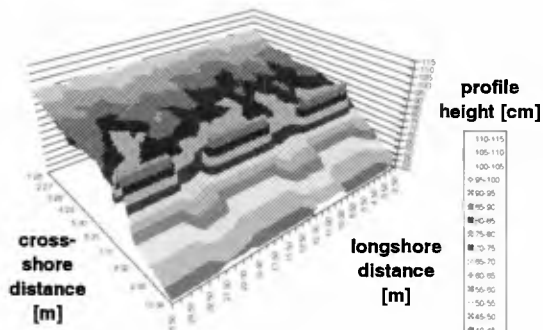


Figure 4. Measured currents, magnitude and direction

The velocity measurements show offshore directed currents towards and through the gaps between the breakwater segments. This leads to significant sediment losses, as illustrated by Figure 5 which shows the bathymetry of the basin with three breakwater segments after 7:30 h of wave action.

Figure 5. Measured bathymetry after 7:30 h of wave action



### 3. 2DH Morphological Modelling, phase averaged

In 1997, a first attempt was made to reproduce the experiments with a numerical model (Schaap 1997, Torrini 1997, Van der Biezen et al. 1997). The package used for this study was Delft3D, developed by Delft Hydraulics. Delft3D consists of several modules, which can be combined so that it suits the case of interest. Only a few aspects of this previous study are mentioned, more details can be found in the given references.

#### 3.1 The model system

Without going into detail (details on Delft3D can be found in the Manual, 1996) the combination of modules applied in this first study is given in Figure 6.

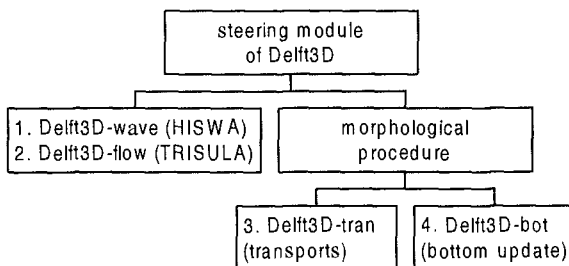


Figure 6. Model system including a wave field module

The computation starts with the calculation of the stationary wave field (module 1) for the given boundary conditions and initial bathymetry. Wave diffraction, which is not included in this module, is represented by directional spreading. Relevant output of module 1 (e.g. wave forces) is written to a communication file. Secondly, the currents are calculated by module 2, which needs information from the communication file. The current field is again written to the communication file. Module 2 takes most of the computation time.

Next the morphological procedure can be run. Module 3 calculates a velocity field from the discharge data in the communication file, with a correction of the total flux velocity for the mass flux by waves. Sediment transports are calculated using the Bijker formula with wave effect. Module 4 updates the bathymetry and adds the new bathymetry to the communication file.

From a stability consideration, the allowed morphological timestep can be determined. Several morphological timesteps can be processed (sequence of modules 3 and 4) without the need to update the current field (and to run module 1 and 2). In this case new velocities corresponding to the updated bottom are calculated from the last discharge data using a continuity relation.

#### 3.2 Waves

The Delft3D-wave module calculates a stationary wave field, which includes wave heights, setup, energy dissipation etc. Figure 7 shows the calculated wave setup for a two-breakwater-segments case. Setup behind the structures is a consequence of energy dissipation by friction and by wave breaking. The resulting setup gradients,

together with the level increase due to mass transport of water over the breakwater crests, are the driving mechanisms for the return flow through the gaps as illustrated in Figure 8.

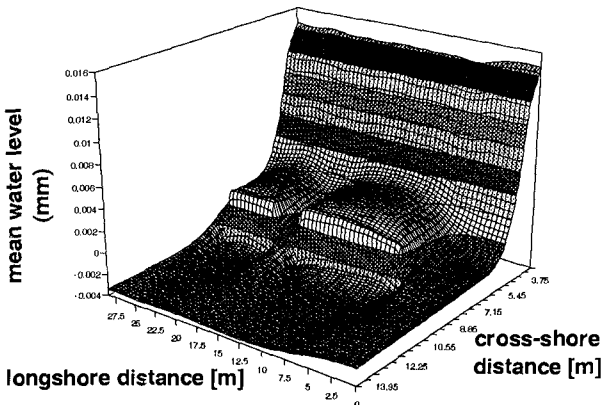


Figure 7. Wave set-up calculated by Delft3D-wave

### 3.3 Currents

The wave forces in the communication file are used to calculate currents. The measured horizontal current pattern, see Figure 4, appears to be well reproduced by the pattern calculated by module 2, see Figure 8. Waves propagate top down; the circulation cells with offshore directed flow through the gaps are clearly present.

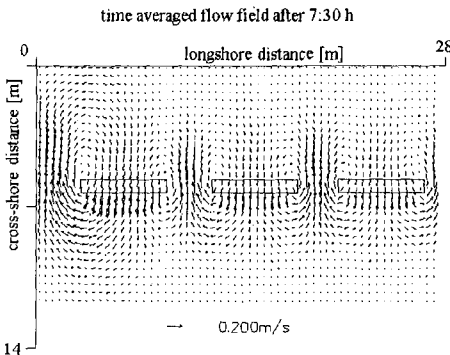


Figure 8. Calculated horizontal current pattern

### 3.4 Morphology

The calculated morphologic changes are, to some extent, in accordance with the measurements. The sediment loss through the gaps between the breakwater segments is well reproduced. However, there are also large discrepancies.

Figure 9 gives the calculated bottom after 3:30 h (approximately half of the experiment duration) which shows large local scour at the waterline and at the landward toe of the structure.

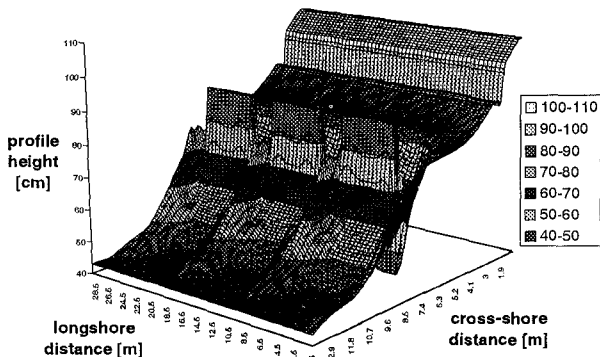


Figure 9. Calculated bathymetry after 3:30 h wave action

The local scour landward of the submerged breakwater follows from a peak in energy dissipation calculated by the wave module. In the experiments, energy was dissipated over a longer distance by spilling breakers. Furthermore, the wave module was not specifically developed to handle a regular wave field.

The unrealistic (computed) scour at the waterline is due to the inability of the model to change 'dry' grid points into 'wet' gridpoints. Since the initial slope is quite steep, this shortcoming has important consequences.

#### 4. 2DH Morphological Modelling, phase resolving

Since the above shortcomings are related to the use of the wave module, and since the experiments are carried out with regular waves, it was decided to try the harmonic boundary option in the flow module for wave generation instead of the wave module. Normally, this option is used to introduce the tide in a simulation.

Delft3D-flow solves the non-linear shallow water (NSW) equations. This implies, amongst others, that a hydrostatic pressure is assumed, which is correct in case of tidal waves. In case of short waves this is usually not so, since vertical accelerations in the water column disturb the hydrostatic pressure.

The waves generated in the basin, however, approximate shallow water waves to a large extent. In the deepest part of the wave basin, the wave celerity that follows from the linear wave theory (with hyperbolic functions) equals 1.99 m/s. The shallow water wave celerity, calculated by the model, equals 2.36 m/s which is only 19% too high. This percentage will even be less in the area of interest, near the structures.

An alternative to the nonlinear shallow water equations, solved in this study, are the Boussinesq equations which can be applied to a larger part of the coastal region. An advanced model based on these equations is discussed by Madsen et al. (1997). In the present study, however, a NSW approach was chosen for the reason that sediment transports and morphology needed to be included.

#### 4.1 The model system

The model system as described in section 3.1 is now changed, since the wave module will not be used during computation. The new model system is given in Figure 10.

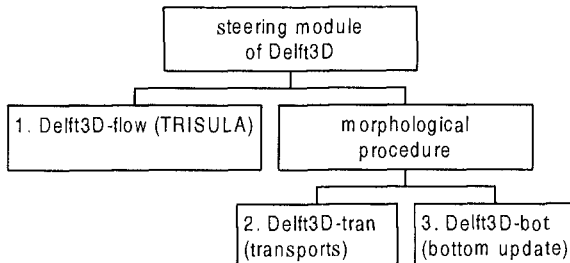


Figure 10. Model system without wave module

In the sections below, the output of each module will be discussed according to their computational sequence during a model run.

#### 4.2 Waves

The simulation starts with the calculation of the wave propagation in the basin (with initial bathymetry) induced by a harmonic boundary condition. In contrast with the previous study, the output does not consist of one stationary wave field. Instead, for each grid point now a time series containing water levels and current data is written to the communication file.

Consequently, the flow in the basin is not calculated separately, like in the previous study, but follows directly from the time-averaged velocity fields stored in the communication file. The same holds for the setup (time averaged water levels).

The calculation of wave propagation is continued until any start-up effects have disappeared. Figure 11 gives an example of calculated water levels in a particular cross-section at different time steps just after the start of a simulation.

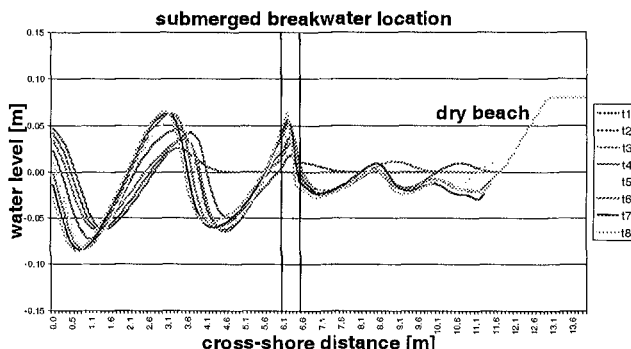


Figure 11. Calculated water levels for different time steps

The influence of the submerged breakwater on the wave height is clearly visible in Figure 11. It is remarked that this approach also includes wave reflection, wave diffraction and, most important, wave runup. Wave runup is responsible for erosion of the dry beach.

The front of the waves tends to become steeper during their propagation towards the breakwaters. To ensure that the wave, once it reaches the structure, has a proper shape, the incoming wave at the boundary was modified to anticipate for the steepening of the wave front. Furthermore, a discharge boundary instead of a water level boundary was chosen since it corresponds more to the motion of the wave paddles.

The parameters used for calibration are the horizontal viscosity and the roughness length. The viscosity was found to be smaller than the default value and the roughness length needed to be enlarged:  $v_H = 0.01 \text{ m}^2/\text{s}$  and  $k_s = 0.5 \text{ m}$ , where  $k_s$  is the Nikuradse roughness length used in White Colebrook's friction formulation. Specially  $k_s$  is large, to obtain enough wave decay. Figure 12 shows some calibration results for a section with and a section without a submerged breakwater.

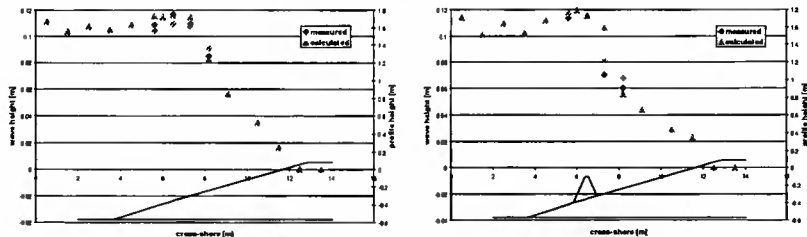


Figure 12. Measured and calculated wave heights

Figure 12 shows that the measured wave heights are reproduced quite well; the calibration parameters are somewhat out of range, though. Some wave height variation seawards of the submerged structure can be seen. This is due to reflection of wave energy. The calculated wave set-up shows the presence of interfering waves, both in cross-shore and in longshore direction, see Figure 13. The waves propagate from left to right in this figure and two submerged breakwater segments are present.

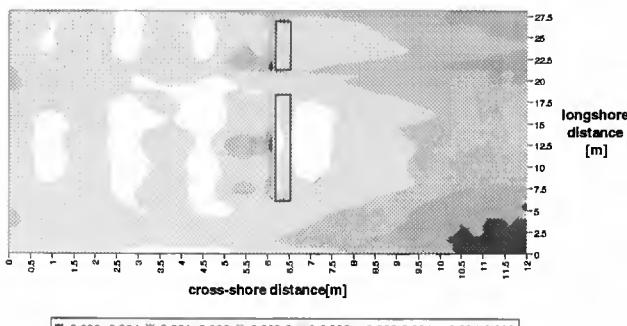


Figure 13. Wave setup [m] calculated from water level time series

Figure 13 also shows a wave setup landwards of the submerged breakwaters, which is in accordance with the output of the wave module in the previous study, see Figure 7 in section 3.2.

#### 4.3 Currents

As mentioned before, the net current pattern as well as the setup can be obtained by averaging respectively the velocity and water level time series over a number of wave periods. The resulting net current pattern looks similar to Figure 8.

#### 4.4 Transports

The sediment transports are computed from discharge fields, stored in the communication file. With use of the bathymetry, first time varying velocity fields are computed from which time varying sediment transports can be calculated. To obtain the net sediment transports, again a time average over a number of wave periods is taken.

The Bijker sediment transport formula is used to calculate sediment transports from the velocity components. However, since the wave module is not used, no wave effect could be included. This reduces the Bijker transport formula to a combination of the Kalinske-Frijlink formula for bed load transport, the Rouse-Einstein expression for the sediment concentration distribution and the Einstein expression for the suspended sediment transport. Since this combined formula is applied within the wave periods (intra-wave), the wave effect is more or less included via the individual discharge fields.

An example of an intra-wave sediment transport field is given in Figure 14.

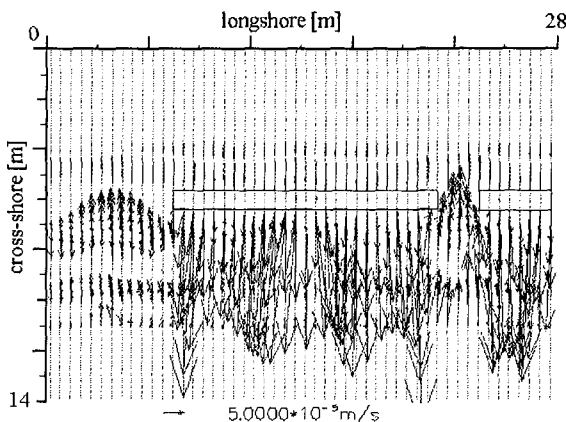


Figure 14. An individual intra-wave sediment transport field

The waves propagate top-down in this figure. Large onshore sediment transports can be seen at the lee side of the structures and offshore transports through the gaps. Other sediment transport fields show a similar pattern.

#### 4.5 Morphology

As mentioned before, one of the advantages of the present NSW approach is the calculation of wave runup. This opens a way to include erosion near and above the waterline.

The transport module uses a parameter that influences the downslope transport by gravity. A higher parameter value yields a smoother profile. Also, a high value increases the transport of sediment from dry to wet grid points near the water line, because at the water line steep slopes tend to occur. As soon as the begin and end grid point of a local slope are both wet, downslope sediment transport takes place. For one cross-section, the profile development including the calculated behaviour near the waterline is given in Figure 15.

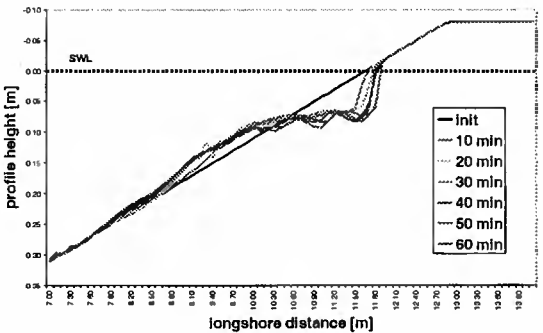


Figure 15. Calculated profile development

With the adjusted parameter for downslope sediment transport, full morphologic runs were made. Since the required computation time is large, only the first 3:30 h of the total duration of the experiments was computed. The runs presented here all have an initial wave height of 0.12 m.

Figure 16 shows the calculated erosion and accretion during a 3:30 h simulation with two submerged breakwaters.

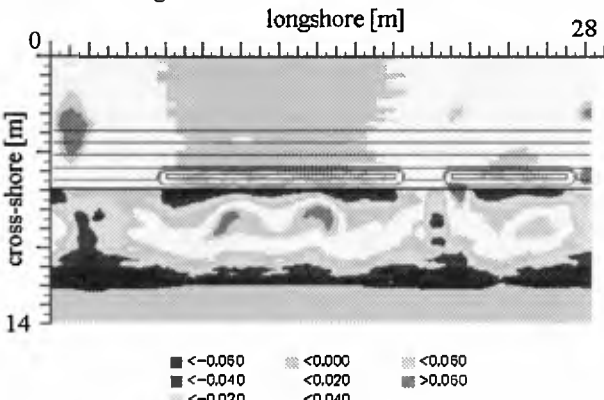


Figure 16. Calculated erosion and sedimentation after 3:30 h

In this figure, erosion is negative and accretion is positive. The figure shows erosion at the waterline and at the landward toe of the submerged breakwaters. Accretion occurs in the area between the structures and the waterline, because of the 'flattening' of the initial profile which is quite steep (1:15). Furthermore, sediment is deposited seawards of the gaps.

Figure 17 shows a 3D image of the calculated bathymetry after 3:30 h wave action with two submerged breakwaters.

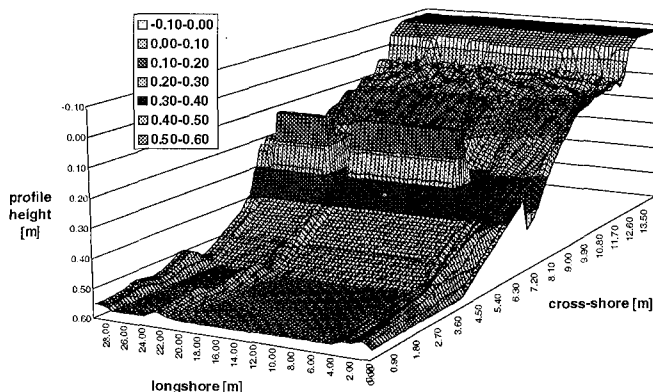


Figure 17. Calculated bathymetry after 3:30 h for two submerged breakwaters

Comparing Figure 17 to Figure 9, it can be seen that the results have improved, specially near the water line and near the landward toe of the structures. The large scouring at these locations, pictured in figure 9, does not occur for the new model system with the shallow water approach. Furthermore, the longshore bed variations, which were absent in the previous study, see Figure 9, are now reproduced.

Finally, the Figures 18a and 18b compare the measured profile, the calculated profile from the previous study and the calculated profile from the present study for two cross-sections. One section is with a submerged breakwater and one section is without a submerged breakwater. The simulated time is 3:30 h.

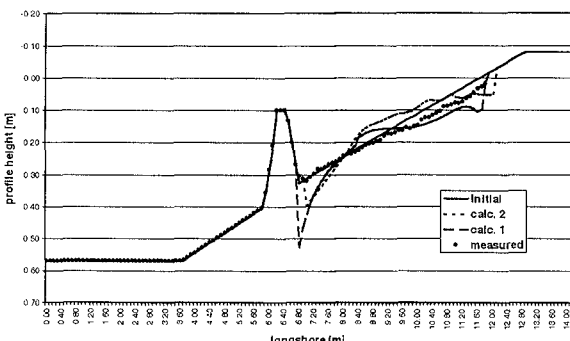


Figure 18a. Comparison for a section with submerged breakwater



Figure 18b. Comparison for a section without submerged breakwater

Specially at the waterline and at the landward toe of the structure, the shallow water approach seems to be more accurate.

### 5. Conclusions and Recommendations

From the above presented numerical study on segmented submerged breakwaters, the following conclusions can be drawn:

- Numerical modelling of submerged breakwaters describing waves with the non-linear shallow water equations yields promising results. The calculation time, however, increases compared to simulations which use a stationary wave field.
- The measured wave height decay over a submerged breakwater is predicted well when using the shallow water approach, although somewhat unusual values have to be used for bottom roughness and horizontal viscosity.
- When modelling morphology around submerged breakwaters, it is of importance to describe the erosion near the water line correctly. The study shows that the intra-wave approach is more accurate on this aspect. However, both approaches require further study.

The shallow water assumption opens new possibilities regarding morphological modelling of submerged breakwaters. The present research has been a pilot study into this field. A lot of fine tuning still needs to be done. Other sediment transport formulas should be tried, and the description of the transport processes near the water line needs more attention. Furthermore, extra measurement data bases would be useful for calibration purposes.

### 6. Acknowledgements

The author wishes to acknowledge Delft Hydraulics for the use of the Delft3D package. The experiments were carried out in the scope of the 'Dynamics of Beaches' project, funded by the Human Capital and Mobility Programme of the Commission of the European Communities (contract CHRX-CT93-0392). The numerical study was partly funded by the MaST-3 project "Surf and swash zone mechanics" (SASME).

## 7. References

- Browder, A.E., R.G. Dean and R. Chen (1996), *Performance of a submerged breakwater for shore protection*, Proc. ICCE'96, Chapter 179.
- De Later, J. (1996), *Effect of submerged breakwaters on a beach profile exposed to regular waves in a wave basin*, Delft University of Technology, Msc.Thesis.
- Høgedal, M. et al. (1994), *Dynamics of Beaches*, Test Definition Report for the Human Capital and Mobility Programme.
- Lamberti, A. and A. Mancinelli (1996), *Italian experience on submerged barriers as beach defence structures*, Proc. ICCE'96, Chapter 182.
- Liberatore, G. (1992), *Detached breakwaters and their use in Italy*, Proc. of the Short Course on Design and Reliability of Coastal Structures, Venice, pp. 373 - 395.
- Madsen, P.A., O.R. Sørensen, H.A. Schäffer (1997), *Surf zone dynamics simulated by a Boussinesq type model. Part II: surf beat and swash oscillations for wave groups and irregular waves*, Coastal Engineering 32, pp. 289 – 319.
- Manual (1996), *An introduction to Delft2D-Mor*, Release 2.07, Delft Hydraulics.
- Murphy, J., A.W. Lewis, C. Wall, J. van de Graaff and S.C. van der Biezen (1996), *Submerged breakwaters research in the EU Human Capital and Mobility Programme*, Proc. of the Maff Conf. on River and Coastal Eng., Hydraulic and Maritime Research Centre Cork.
- Nobuoka, H., I. Irie, K. Hajime and N. Mimura (1996), *Regulation of nearshore circulation by submerged breakwater for shore protection*, Proc. ICCE'96, Chapter 185.
- Ozaki, T. and K. Mitsuhashi (1993), *Ecology conscious submerged breakwater*, Proc. of the Symp. on coastal and ocean management, ASCE, pp. 265 – 279.
- Schaap, J. (1997), *Modelling the effects of submerged breakwaters in a wave basin*, Delft University of Technology, Msc.Thesis.
- Smith, D.A.Y., P.S. Warner, R.M. Sorensen, L.A. Nurse and K.A. Atherley (1995), *Submerged-crest breakwater design*, Proc. 1995 Coastal Struct. Conf., London.
- Tomasicchio, U.(1996), *Submerged breakwaters for the defence of the shoreline at Ostia, field experiences, comparison*, Proc. ICCE'96, Chapter 186.
- Torrini, L. (1997), *Nearshore effects of submerged breakwaters*, Delft University of Technology, Msc.Thesis.
- Van der Biezen, S.C., J. van de Graaff and J. de Later (1996), *3D model tests of the influence of submerged breakwaters on a beach profile exposed to regular waves*, Proc. PECS'96, The Hague.
- Van der Biezen, S.C., J. van de Graaff, J. Schaap and L. Torrini (1997), *Small scale tests and numerical modelling of the hydrodynamic and morphological effects of submerged breakwaters*, Proc. Pacific Coasts and Ports, pp. 219 – 224.